Journal of Organometallic Chemistry 897 (2019) 64–69

Contents lists available at ScienceDirect

Journal of Organometallic Chemistry

journal homepage: www.elsevier.com/locate/jorganchem

Co(cyclam) alkynyl complexes of *gem*-DEE-aryl: Synthesis, molecular and electronic structures

Tyler J. Azbell, Susannah D. Banziger, Brandon L. Mash, Tong Ren*

Department of Chemistry, Purdue University, West Lafayette, IN, 47906, USA

ARTICLE INFO

Article history:
Received 1 June 2019
Received in revised form
21 June 2019
Accepted 24 June 2019
Available online 27 June 2019

Keywords:
Cobalt
Cyclam
Alkyne
Cross conjugation

ABSTRACT

Reported in this contribution are the syntheses of mono-alkynyl complexes [Co(cyclam)(*gem*-DEE-Ar)Cl]Cl (cyclam = 1,4,8,11-tetraazacyclotetradecane; *gem*-DEE = *geminal*-diethynylethene) with Ar as either $-C_6H_4$-4-NO_2 (**1**) or $-C_6H_4$-4-NMe_2 (**2**) from the reactions between $[Co(cyclam)Cl_2]Cl$ and H-*gem*-DEE-Ar under weak base conditions. Further reaction between compound **1** and Li-*gem*-DEE$-C_6H_4-$4-NMe_2 at −78 °C afforded the unsymmetric complex *trans*-[Co(cyclam)(*gem*-DEE$-C_6H_4-$4-NO_2)(*gem*-DEE$-C_6H_4-$4-NMe_2)]Cl (**3**). Providing structural features observed for other Co(cyclam) alkynyls, X-ray diffraction study also reveals the influence of the aryl substituent on the first coordination sphere of the Co(III) center. The presence of an aryl substituent also shifts the Co-based redox couples, and enables intense LMCT transitions that are absent in complexes of unsubstituted *gem*-DEE. These contrasts can be rationalized based on DFT calculations.

1. Introduction

The electronic structures of metal alkynyl compounds and the opto-electronic characteristics displayed by these compounds have long fascinated inorganic and materials chemists [1–6]. *Linearly* conjugated metal alkynyl compounds have been of great interest as the scaffold for molecular wires due to both structural rigidity and extensive π-conjugation [7–10]. Furthermore, these compounds may undergo one or more reversible one-electron metal-centered redox events, which enable the assessment of the degree of charge delocalization along a metal-alkynyl backbone using the mixed valency model [11–13]. Earlier demonstrations of substantial electronic delocalization include the C_4-bridged diiron compounds by Lapinte [14], the C_4-bridged dirhenium compounds by Gladysz [15], which were followed by the C_4-bridged diruthenium compounds [16] and the C_4- and C_8-bridged dimers of diruthenium compounds [17,18]. Equally significant is the electronic delocalization *across* metal centers, which is often evaluated by the $(Fc-Fc)^+$ mixed valency in the *trans*-FcC_{2n}-[M]-$C_{2n}Fc$ type compounds, as exemplified by the cases with M as Pt [19], Ru [20], Ru_2 [21,22] and Os-carbonyl clusters [23,24]. Though more challenging and hence less studied, single molecule conductance of linear metal alkynyls have been measured utilizing various nano-junction techniques with M as Pt [25], Ru [26–29], and Ru_2 [30,31]. Functional molecular devices, such as photo-addressable switching junction [32] and charge injection (flash) memory devices [33], have been realized as well.

Compared to linearly conjugated metal alkynyls, transition metal compounds based on cross-conjugated alkynyl ligands remains underexplored. Cross-conjugation is defined as the conjugation of two unsaturated π-segments that are conjugated with an intervening unsaturated moiety, but not to each other [34]. Due to their unique iso-electronic partition (bifurcation), cross-conjugated molecules are interesting targets in attenuating electron delocalization [35]. Owing to the facile and high yield protocols developed by Diederich [36] and Tykwinski [37–41], *geminal*-diethynylethene (*gem*-DEE, Chart 1) has become a favorite metallation target. The first examples of metal containing *gem*-DEE compounds are those based on Pt(II) complexes by Tykwinski and coworkers [42,43]. Recent years have seen a heightened interest in using *gem*-DEE or its analogue as the bridge in bimetallic compounds ([M]-*gem*-DEE-[M]) with [M] as Cp*Ru(dppe) [44,45], $CpRu(PPh_3)_2$ [46], and ferrocenyl [47,48]. Our laboratory initially explored *gem*-DEE compounds based on $Ru_2(DMBA)_4$ (DMBA = *N,N′*-dimethylbenzamidinate) [49,50] and $Ru_2(ap)_4$ (*ap* = 2-anilinopyrdinate) species [51]. To circumvent the instability encountered in Ru_2 based compounds, especially that of $[Ru_2(ap)_4]_2$(μ-*gem*-DEE), our attention was shifted to *gem*-DEE compounds based on M(cyclam) (cyclam = 1,4,8,11-

* Corresponding author.
E-mail address: tren@purdue.edu (T. Ren).

https://doi.org/10.1016/j.jorganchem.2019.06.031
0022-328X/

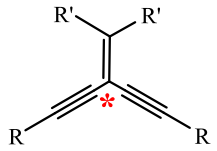

Chart 1. Acyclic cross-conjugated *gem*-DEE motif; * indicates the bifurcation point.

tetraazacycloctetradecane) [52,53]. To this end, *trans*-[M(cyclam)(-*gem*-DEE)$_2$]$^+$ type compounds have been prepared and thoroughly characterized with M as Cr(III) [54] and Fe(III) [55]. Both the *trans*-[Co(cyclam)(*gem*-DEE)(C$_2$R)]$^+$ and *trans*-[Co(cyclam)Cl]$_2$(μ-*gem*-DEE) type compounds were prepared as well [56–58], and the latter compounds are the first structural examples of bimetallic species bridged by *gem*-DEE.

As a departure from the efforts on the symmetric *trans*-[M(cyclam)(*gem*-DEE)$_2$]$^+$ type compounds, we report herein the synthesis of mono-alkynyl *trans*-[Co(cyclam)(*gem*-DEE-Ar)Cl]Cl compounds with Ar as −C$_6$H$_4$-4-NO$_2$ (**1**, Scheme 1) and −C$_6$H$_4$-4-NMe$_2$ (**2**), and subsequent conversion of **1** to unsymmetric *trans*-[Co(cyclam)(*gem*-DEE−C$_6$H$_4$−4-NO$_2$)(*gem*-DEE−C$_6$H$_4$−4-NMe$_2$)]Cl (**3**). Also described are the voltammetric characterization of all three new compounds and the structural elucidation of compounds **1** and **2**.

2. Results and discussion

2.1. Syntheses

The preparation of mono-alkynyl species **1** and **2** drew inspiration from the recent work of Shores and coworker, who demonstrated high yield formation of [Co(cyclam)(C$_2$Ph)Cl]$^+$ from refluxing [Co(cyclam)Cl$_2$]Cl and HC$_2$Ph in the presence of Et$_3$N [59]. This protocol has been successful in yielding a variety of [Co(cyclam)(*gem*-DEE-R)Cl]$^+$ compounds in our laboratory [56,57]. Thus, the reaction of [Co(cyclam)Cl$_2$]Cl and TMS-*gem*-DEE−C$_6$H$_4$−4-NMe$_2$ in THF/MeOH (v/v, 1:4) and Et$_3$N under reflux resulted in compound **2** in 47% yield (based on Co). Since TMS-*gem*-DEE−C$_6$H$_4$−4-NO$_2$ did not undergo desilylation in the presence of Et$_3$N, it was converted to H-*gem*-DEE−C$_6$H$_4$−4-NO$_2$ using K$_2$CO$_3$ in methanol, and the crude extract was used to react with [Co(cyclam)Cl$_2$]Cl to yield compound **1** (43% based on Co). Introduction of the second *gem*-DEE−C$_6$H$_4$−Ar' ligand is more challenging and the reaction between *trans*-[Co(cyclam)(*gem*-DEE-Ar)(NCMe)]$^{+2}$ (prepared according to our recently published procedure [60]) only led to dissociation of the Co-bound *gem*-DEE-Ar in the starting material. Previously, it was shown that the room temperature reaction between [Co(cyclam)(C$_2$R)Cl]$^+$ and LiC$_2$R′ resulted in the desired [Co(cyclam)(C$_2$R)(C$_2$R′)]$^+$ compound in low yield along with significant alkynyl scrambling byproducts [61]. It was discovered more recently that alkynyl scrambling was avoided in such a reaction when carried out at −78 °C, and the desired [Co(cyclam)(C$_2$R)(C$_2$R′)]$^+$ products were isolated in yields as high as 50% [62]. Thus, the treatment of **1** with Li-*gem*-DEE−C$_6$H$_4$−4-NMe$_2$ in THF at −78 °C led to the formation of **3** in 19% yield, post purification. All three new compounds are diamagnetic and are orange (**1** and **3**) or red (**2**) crystalline materials, consistent with a low spin Co(III) center. They were characterized with FT-IR and ^{1}H NMR spectroscopic techniques, with latter providing spectra with diagnostic peaks.

2.2. Molecular structures

X-ray quality single crystals for complex [**1**]$^+$ were grown after in situ counter-ion exchange from Cl$^-$ to BPh$_4^-$ (with NaBPh$_4$) using slow diffusion of hexanes into EtOAc. Single crystals of compound **2** were obtained through slow diffusion of ether into a concentrated methanol solution. Molecular structures of complex ions [**1**]$^+$ and [**2**]$^+$ are shown in Figs. 1 and 2, respectively, while the selected bond lengths and angles are collected in Table 1. The Co centers assume a pseudo-octahedral geometry with the *gem*-DEE and Cl ligands *trans*-to each other. The geometric parameters for the *gem*-DEE fragment are very similar in **1** and **2**, and are in good agreement with those observed for previously published Co-*gem*-DEE species [56,57]. A closer comparison of data for [**1**]$^+$ and [**2**]$^+$ reveals subtle but interesting structural contrasts that are dependent on the electron donating/withdrawing nature of the aryl substituent (inductive effect instead of π-conjugation). The Co−C bond in [**2**]$^+$ is shorter than that in [**1**]$^+$, reflecting an enhancement of Co-*gem*-DEE interaction with a donor substituent. Stronger Co−C bond in [**2**]$^+$ results in a longer Co−Cl bond than that of [**1**]$^+$, a

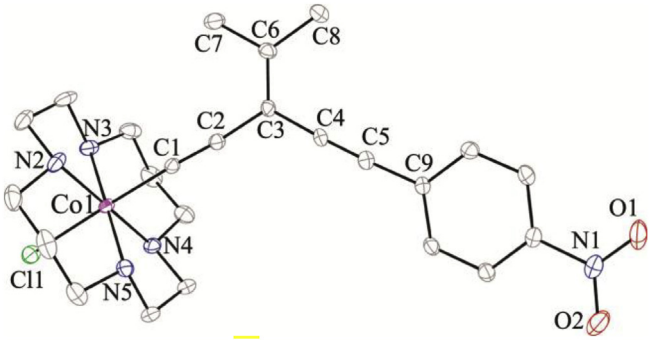

Fig. 1. ORTEP plot of compound [1]$^+$ at 30% probability level; BPh$_4^-$, hydrogen atoms, and solvent molecules were omitted for clarity.

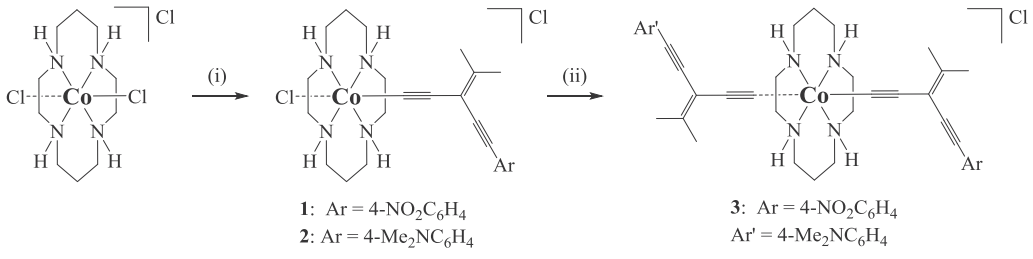

1: Ar = 4-NO$_2$C$_6$H$_4$
2: Ar = 4-Me$_2$NC$_6$H$_4$

3: Ar = 4-NO$_2$C$_6$H$_4$
Ar' = 4-Me$_2$NC$_6$H$_4$

Conditions: (i) Me$_3$Si-*gem*-DEE-C$_6$H$_4$-4-NO$_2$; Et$_3$N, MeOH/THF; 60 °C, 16 h; (ii) **1**, Li-*gem*-DEE-C$_6$H$_4$-4-NMe$_2$; -78 °C, THF.

Scheme 1. Synthesis of compounds **1**, **2** and **3**.

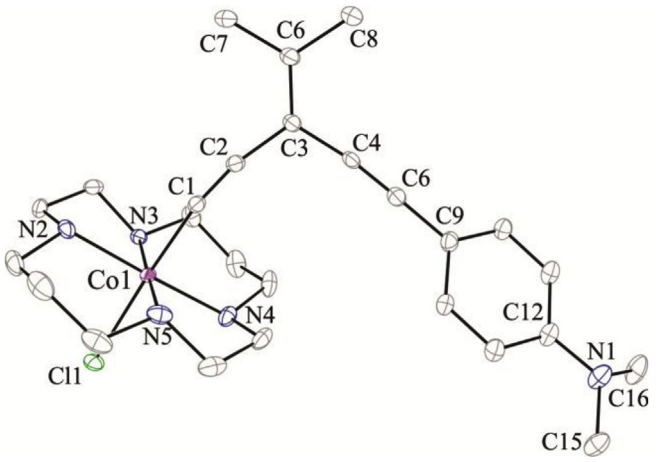

Fig. 2. ORTEP plot of compound $[2]^+$ at 30% probability level; Cl^-, hydrogen atoms, disorder, and solvent molecules were omitted for clarity.

Table 1
Selected bond lengths (Å) and angles (°) for complexes $[1]^+$ and $[2]^+$.

	$[1]^+$	$[2]^+$
C1–Co1	1.884 (4)	1.873 (3)
Cl1–Co1	2.313 (1)	2.319 (1)
N2–Co1	1.968 (4)	1.945 (4)
N3–Co1	1.983 (4)	1.997 (4)
N4–Co1	1.957 (4)	1.999 (3)
N5–Co1	1.965 (4)	1.972 (3)
C1–C2	1.216 (6)	1.203 (4)
C2–C3	1.447 (6)	1.442 (4)
C3–C6	1.359 (6)	1.353 (4)
C3–C4	1.434 (6)	1.433 (4)
C4–C5	1.202 (6)	1.207 (4)
C5–C9	1.438 (6)	1.446 (8)
C6–C7	1.492 (7)	1.494 (4)
C6–C8	1.501(7)	1.499 (4)
C1–Co1–Cl1	176.2 (2)	177.39 (8)
C2–C1–Co1	176.1 (4)	171.2 (2)
C1–C2–C3	175.1 (5)	168.6 (3)
C4–C3–C2	118.6 (4)	112.3 (2)
C5–C4–C3	177.5 (5)	172.9 (3)
C12–N1–C15	–	119.0 (4)
C12–N1–C16	–	120.4 (4)
C15–N1–C16	–	114.0 (4)

manifestation of the *trans*-influence. In addition, the increase of electron density at the Co center in **[2]**$^+$ led to longer Co–N bonds (averaged bond length: 1.978 [4] Å), while the electron deficient complex **[1]**$^+$ has shorter Co–N bonds (averaged bond length: 1.968 [4] Å).

2.3. Electrochemistry

The redox characteristics of compounds **1**, **2** and **3** were examined with cyclic voltammetry, and the results are shown in Fig. 3. Similar to previously studied Co(cyclam) alkynyls [52,53], all three compounds display two irreversible one-electron processes centered at Co(III): an oxidation (**A**) and a reduction (**B**). The irreversibility of the former is attributed to the fact that the occupied *d* orbitals of Co(III) center (t_{2g}^6) are deeply buried. The reduction (**B**) necessitates the occupation of d_{z2} orbital, which usually results in the dissociation of one of the axial ligands, Cl^- in the case of mono-alkynyl and an alkynyl in the case of bis-complexes, and hence the irreversibility. Dependence of CVs on the aryl substituent is clear from the comparison of **1** and **2**: the strong electron withdrawing

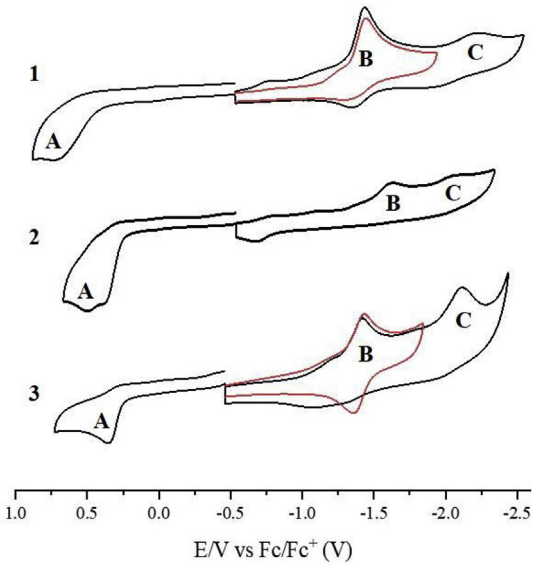

Fig. 3. Cyclic voltammograms of 1, 2, and 3 in 0.1 M MeCN solution of Bu_4NPF_6 at a scan rate of 100 mV/s.

nature of *p*-NO_2 renders easier reduction (low E_{pc} for **B**) and harder oxidation (very positive E_{pa} for **A**) in complex **1**, while the opposite is true for **2**. The electrode potentials of complex **3** do not follow this trend since it is a bis-alkynyl species and significantly electron richer, as exemplified by the least positive E_{pa}(**A**). All three compounds also display a second Co reduction which is irreversible as well (Table 2).

2.4. Electronic absorption spectra

UV–Vis absorption spectra of compounds 1–3 are shown in Fig. 4. The UV region feature π –> π* transitions that are localized on the gem-DEE-Ar ligands. Fairly intense shoulders are present in the visible region as well, and are likely of LMCT nature. Such transitions likely originate from the π(gem-DEE-Ar) in 1 (ca. 355 nm) and 3 (ca. 370 nm), but from the lone pair (n) of NMe2 in 2. Since the n(NMe2) is higher in energy than π(gem-DEE-Ar), this peak (ca. 400 nm) in 2 is significantly red shifted from those of 1 and 3. It is noteworthy that such intense absorption bands were not observed for the [Co(cyclam)(gem-DEE-R)Y]+ type compounds (R = SiR′3 or H; Y = Cl or C2R″) [57], which reinforces the above-mentioned LMCT assignment for the current series. Linear Co(cyclam) species bearing -C2C6H4-4-NO2 [61] or -C2C6H4-4-NMe2 [60] alkynyl ligands also possess strong LMCT transitions ca. 340 nm and ca. 330 nm, respectively. Also, the d-d bands for the [Co(cyclam)(gem-DEE-R)Y]+ type compounds were detected around 490 nm with the value of ε around 100. Clearly, these weak d-d bands were overshadowed by the LMCT bands in compounds 1–3.

2.5. Electronic structures via DFT calculations

To elaborate on the orbital interactions between the aryl substituents and Co center in **[1]**$^+$ and **[2]**$^+$, and potential interactions

Table 2
Electrode potentials of observed redox couples (V) in compounds 1, 2, and 3.

	E_{pa} (A)	E_{pc}(B)	E_{pc} (C)
1	0.73	−1.43	−2.20
2	0.50	−1.62	−2.10
3	0.37	−1.45	−2.14

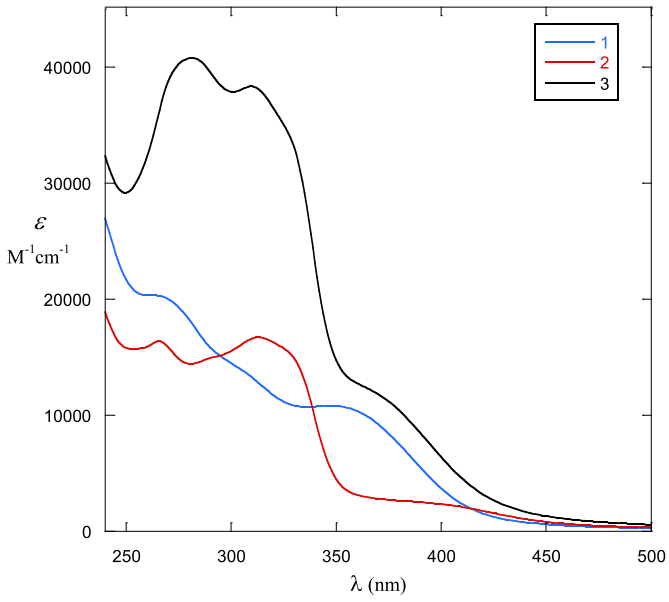

Fig. 4. UV–Vis absorption spectra of compounds 1–3 recorded in MeOH.

between two aryl substituents in **[3]**$^+$, spin-restricted density function calculations at B3LYP using the LanL2DZ basis set for Co and def2-SVP basis set for all other atoms in Gaussian Suite 16 were performed for all three complexes. In complex **[1]**$^+$, the HOMO is dominated by the out of plane *gem*-DEE π orbital ($\pi_\perp$) [35,63] with additional contributions from $-C_6H_4$-4-NO_2 and very minor d_{xz}, while the LUMO is predominantly the Co $3d^{22}_{x\text{-}y}$ with contribution from nitrogens of the cyclam ring. In **[2]**$^+$, the HOMO is mostly the π orbital of C_6H_4-4-NMe_2 with $\pi_\perp$ of *gem*-DEE being secondary, while the LUMO is mostly the Co $3d^{22}_{x\text{-}y}$ as in **[1]**$^+$. The HOMO energy level of **[1]**$^+$ is significantly lower than **[2]**$^+$, because of the strong electron withdrawing ability of C_6H_4-4-NO_2 group. The Co t_{2g} set is deeply buried in both **[1]**$^+$ and **[2]**$^+$, similar to the finding of DFT studies of related Co(cyclam) alkynyls [56–58]. In complex **[3]**$^+$, the HOMO lies entirely on the *gem*-DEE–C_6H_4–4-NMe_2, while the LUMO+1 is located mostly on the C_6H_4-4-NO_2 group with a minute contribution of $\pi_\perp$ of *gem*-DEE. This electronic separation correlates to the assignment of the two ligands as electron donating and electron withdrawing respectively. (see Fig. 5).

3. Conclusions

Three unique cross conjugated Co^{III} complexes have been prepared based on the *gem*-DEE-Ar type ligands, and the success in isolating the unsymmetric complex **3** is especially noteworthy. Both the structural features of **1** and **2** and voltammetric behaviors of **1**–**3** reveal subtle but significant impact of the electron donating/withdrawing aryl substituents, which has been further corroborated by the DFT analysis. Future work will focus on expanding this motif to include more complex *gem*-DEE-Ar ligands as well as ways to modify the reaction conditions to increase yield.

4. Experimental

4.1. General procedures

4.1.1. Materials

n-Butyl lithium was purchased from Sigma-Aldrich and dry acetonitrile was purchased from ACROS Chemical. All reagents were used as received. [Co(cyclam)Cl_2]Cl was prepared according to literature procedures [64]. TMS-*gem*-DEE–C_6H_4–4-NO_2 and TMS-*gem*-DEE–C_6H_4–4-NMe_2 were also synthesized according to literature procedure [38,39]. Tetrahydrofuran (THF) was distilled over Na/benzophenone under a dry N_2 atmosphere. All reactions were carried out under N_2 using standard Schlenk line techniques.

4.1.2. Physical measurements

UV–Vis–NIR spectra were obtained with a JASCO V-670 UV–Vis–NIR spectrophotometer. Infrared spectra were obtained on a JASCO FT-IR 6300 spectrometer via ATR on a ZnSe crystal. ^{1}H NMR spectra were recorded on a Varian INOVA300 NMR with chemical shifts (δ) referenced to the solvent signal (CD_3OD at 4.88 and 3.31 ppm). Electrospray Ionization Mass Spectrometry (ESI-MS) spectra were recorded using an Advion Mass Spectrometer. Elemental analysis was performed by Atlantic Microlab, Inc in Norcross, GA. Cyclic voltammograms were recorded in 0.1 M n-Bu_4NPF_6 and 1.0 mM concentrations of cobalt species in dry acetonitrile under Ar. A CHI620A voltammetric analyzer with a glassy carbon working electrode (diameter = 2 mm), Pt-wire counter electrode, and Ag/AgCl reference electrode with ferrocene used as an external reference ($E_{1/2}$ = 0.49 V, MeCN).

4.2. Preparation of [Co(cyclam)(gem-DEE-C6H4-4-NO2)Cl]Cl (1)

In a round bottom flask, 336 mg (1.13 mmol) of TMS-*gem*-DEE–C_6H_4–4-NO_2 was dissolved in 20 mL THF/MeOH (1:1). Excess K_2CO_3 was added and the solution stirred at room temperature for 1 h. Solvent was removed and the material was purified over a THF silica plug to yield 100 mg of H-*gem*-DEE-PhNO_2. [Co(cyclam)Cl_2]Cl (150 mg, 0.41 mmol) and Et_3N (1.1 mL) were dissolved in 20 mL of methanol, to which H-*gem*-DEE-PhNO_2 (100 mg, 0.44 mmol) in 5 mL THF was added. The solution was refluxed overnight under N_2 and changed from a deep green solution to a brown solution. After the removal of solvent, the crude mixture was separated using silica gel plug purification. The desired product eluted as an orange band with CH_2Cl_2/MeOH (5:1). The product band was recrystallized using ether/acetone (3:1) and CH_2Cl_2 to yield 98 mg of desired product (43% based on [Co(cyclam)Cl_2]Cl). ESI-MS: **[1]**$^+$, 518.0. ^{1}H NMR (300 MHz, Methanol-d) δ 8.22 (d, J = 8.8 Hz, 2H), 7.60 (d, J = 10.7 Hz, 2H), 5.11 (s, 4H), 2.76–2.51 (m, 10H), 2.22 (s, 3H), 2.14 (s, 3H), 2.09–1.48 (m, 10H). UV–Vis spectra, λ_{max} (nm, ε (M^{-1} cm^{-1})): 347 (10,826). IR (cm^{-1}): C≡C: 2199 (m), 2109 (m). Elem. Anal. Found (Calcd) for $C_{29}H_{44}N_5O_3CoCl_6$ (**1**•2CH_2Cl_2•1$(CH_3)_2CO$): C, 45.47 (45.28); H, 4.99 (5.04); N, 9.1 (8.95).

4.3. Preparation of [Co(cyclam)(gem-DEE-C6H4-4-NMe2)Cl]Cl 2

[Co(cyclam)Cl_2]Cl (100 mg, 0.27 mmol) and Et_3N (0.75 mL) were mixed in 20 mL of methanol, to which TMS- *gem*-DEE–C_6H_4–4-NMe_2 (90 mg, 0.31 mmol) in 5 mL THF was added. The mixture was refluxed for 16 h under N_2, turning from green to red. After the removal of solvent, the crude mixture was purified over silica, with the product eluting as a dark red band with MeOH/EtOAc (1:5). The product band was recrystallized from methanol/CH_2Cl_2 (1:1) and ether to yield 70 mg of dark red product (47% based on [Co(cyclam)Cl_2]Cl). ESI-MS: **[2]**$^+$, 516.0. ^{1}H NMR (300 MHz, Methanol-d) δ 7.20 (d, J = 8.4 Hz, 2H), 6.67 (d, J = 9.0 Hz, 2H), 5.11 (s br 4H), 2.95 (s, 6H), 2.52 (m, 10H), 2.16 (s, 3H), 2.07 (s, 3H), 1.71–1.52 (m, 10H). UV–Vis spectra, λ_{max} (nm, ε (M^{-1} cm^{-1})): 313 (16,706), 406 (2824); IR (cm^{-1}): C≡C: 2094 (m), 2173 (m). Elem. Anal. Found (Calcd) for $C_{27}H_{42}N_5CoCl_4$ (**2**•1CH_2Cl_2): C, 50.24 (50.13); H, 6.58 (6.71); N, 11.08 (11.21).

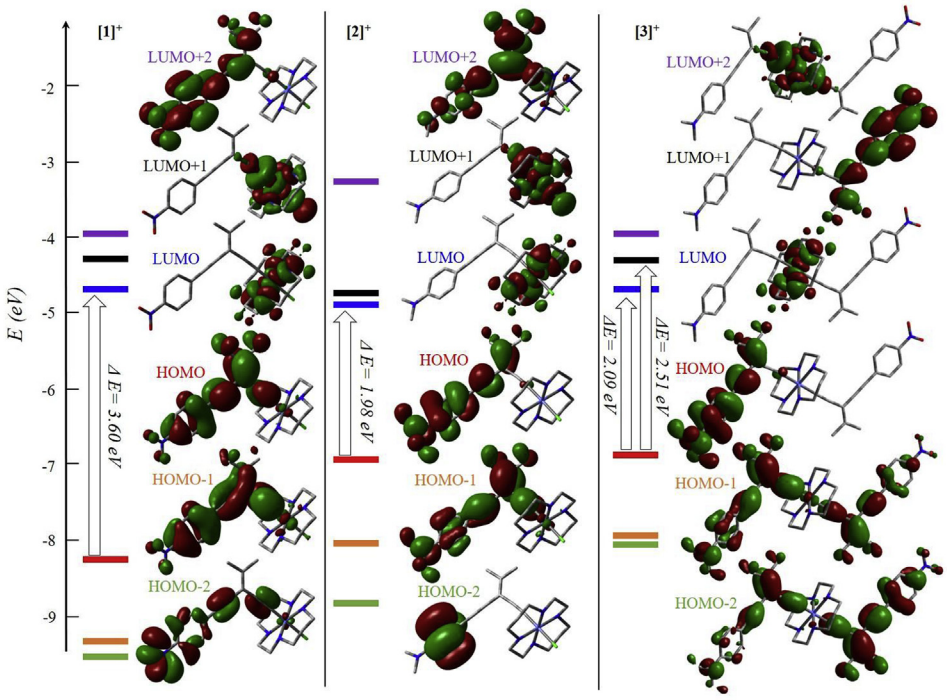

Fig. 5. Molecular orbital diagrams of compounds $[1]^+$, $[2]^+$, and $[3]^+$ obtained from DFT calculations (iso-value 0.020).

4.4. Preparation of [Co(cyclam)(gem-DEE–C_6H_4–4-NO_2) (gem-DEE–C_6H_4–4-NMe_2)]Cl (**3**)

Compound **1** (70 mg, 0.13 mmol) reacted with Li-*gem*-DEE-C_6H_4-4-NMe_2 (0.13 mmol) in 20 mL dry THF at −78 °C to produce a dark purple solution. After 3 h, the reaction was quenched with MeOH and an orange tint arose in the solution. The crude solution was purified on a silica column loaded with MeOH/CH_2Cl_2 (1:5). The orange band was identified as the desired product, isolated, and recrystallized from ether and methanol to yield 18 mg of light orange solid (19% based on **2**). ESI-MS: $[\mathbf{3}]^+$, 705.7. ^{1}H NMR (300 MHz, Methanol-d) δ 8.23 (d, J = 9.0 Hz, 2H), 7.72–7.52 (m, 2H), 7.22 (dd, J = 8.8, 2.8 Hz, 2H), 6.69 (d, J = 8.8 Hz, 2H), 4.60 (s, 4H), 2.96 (s, 6H), 2.68–2.46 (m, 14H), 2.26 (s, 3H), 2.20 (s, 3H), 2.15 (s, 3H), 2.09 (s, 3H), 1.99–1.81 (m, 3H), 1.56–1.37 (m, 3H). UV–Vis spectra, λ_{max} (nm, ε (M^{-1} cm^{-1})): 279 (40,697), 308 (38,283). IR (cm^{-1}): C≡C: 2090 (m), 2196 (m). Elem. Anal. Found (Calcd) for $C_{43}H_{58}N_6O_3CoCl_7$ **3**•3CH_2Cl_2•1H_2O): C, 50.54 (50.46); H, 5.19 (5.27); N, 8.34 (8.39).

Table 3
Experimental crystal data for compounds **1** and **2**.

Compound	1	2
Chemical Formula	$C_{24}H_{34}ClCoN_5O_2 \cdot C_{24}H_{20}B \cdot CH_4O$	$C_{26}H_{41.53}Cl_2CoN_5O_{0.76}$
Formula Weight	870.19	566.22
Space group	$Pna2_1$	$P1$
a, Å	18.6242 (11)	9.5839 (5)
b, Å	12.0982 (7)	11.7809 (5)
c, Å	39.348 (3)	12.3600 (5)
α, °	–	91.349 (3)
β, °	–	94.269 (3)
γ, °	–	93.675 (2)
V, Å^3	8865.9 (9)	1388.24 (11)
Z	8	2
$\Delta\rho_{max}$, $\Delta\rho_{min}$ (e Å^{-3})	1.71, −1.02	0.36, −0.45
λ, Å	0.71073	1.54178
T, K	150	150
$(\sin\theta/\lambda)_{max}$ (Å^{-1})	0.717	0.611
R	0.055	0.043
R_w (F^2)	0.145	0.116

4.5. Computational details

The geometries of **1**, **2** and **3** in the ground state were fully optimized from the crystal structures reported in this work using the density functional method B3LYP (Beck's three-parameter hybrid functional using the Lee–Yang–Parr correlation functional) and employing the LanL2DZ basis set for Co and def2-SVP basis set for all other atoms (C, H, O, N, Cl). Compound **3** was modeled using the crystal structure geometries of the *gem*-DEE ligands from both **1** and **2**. The calculation was accomplished by using the Gaussian16 program package [65].

4.6. X-ray Crystallographic analysis

Single crystal X-ray data was collected on a Bruker AXS D8 Quest CMOS diffractometer with Apex3 software. Data was reduced using SAINT and structures were solved with SHELXTL [66]. Refinement was performed with SHELXL. ORTEP plots were produced using SHELXTL [66].(see table 3)

Acknowledgement

We thank the National Science Foundation for generously supporting this work (CHE 1764347 for research and CHE 1625543 for X-ray diffractometers). SDB thanks Purdue University for a *Cagianas Fellowship*.

Appendix A. Supplementary data

Supplementary data to this article can be found online at https://doi.org/10.1016/j.jorganchem.2019.06.031.

References

[1] R. Nast, Coord. Chem. Rev. 47 (1982) 89.
[2] J. Manna, K.D. John, M.D. Hopkins, Adv. Organomet. Chem. 38 (1995) 79.
[3] M.I. Bruce, Chem. Rev. 98 (1998) 2797.
[4] M.I. Bruce, P.J. Low, Adv. Organomet. Chem. 50 (2004) 179.
[5] C.-L. Ho, Z.-Q. Yu, W.-Y. Wong, Chem. Soc. Rev. 45 (2016) 5264.
[6] A. Haque, R.A. Al-Balushi, I.J. Al-Busaidi, Muhammad S. Khan, P.R. Raithby, Chem. Rev. 118 (2018) 8474.
[7] F. Paul, C. Lapinte, Coord. Chem. Rev. 178–180 (1998) 431.
[8] T. Ren, Organometallics 24 (2005) 4854.
[9] K. Costuas, S. Rigaut, Dalton Trans. 40 (2011) 5643.
[10] J.F. Halet, C. Lapinte, Coord. Chem. Rev. 257 (2013) 1584.
[11] R.J. Crutchley, Adv. Inorg. Chem. 41 (1994) 273.
[12] B.S. Brunschwig, C. Creutz, N. Sutin, Chem. Soc. Rev. 31 (2002) 168.
[13] Y. Tanaka, M. Akita, Coord. Chem. Rev. 388 (2019) 334.
[14] N. Le Narvor, C. Lapinte, J. Chem. Soc., Chem. Commun. (1993) 357.
[15] Y.L. Zhou, J.W. Seyler, W. Weng, A.M. Arif, J.A. Gladysz, J. Am. Chem. Soc. 115 (1993) 8509.
[16] M.I. Bruce, P.J. Low, K. Costuas, J.-F. Halet, S.P. Best, G.A. Heath, J. Am. Chem. Soc. 122 (2000) 1949.
[17] T. Ren, G. Zou, J.C. Alvarez, Chem. Commun. (2000) 1197.
[18] K.-T. Wong, J.-M. Lehn, S.-M. Peng, G.-H. Lee, Chem. Commun. (2000) 2259.
[19] D. Osella, R. Gobetto, C. Nervi, M. Ravera, R. D'Amato, M.V. Russo, Inorg. Chem. Commun. 1 (1998) 239.
[20] Y. Zhu, O. Clot, M.O. Wolf, G.P.A. Yap, J. Am. Chem. Soc. 120 (1998) 1812.
[21] G.L. Xu, M.C. DeRosa, R.J. Crutchley, T. Ren, J. Am. Chem. Soc. 126 (2004) 3728.
[22] G.-L. Xu, R.J. Crutchley, M.C. DeRosa, Q.-J. Pan, H.-X. Zhang, X. Wang, T. Ren, J. Am. Chem. Soc. 127 (2005) 13354.
[23] R.D. Adams, B. Qu, Organometallics 19 (2000) 2411.
[24] R.D. Adams, B. Qu, M.D. Smith, T.A. Albright, Organometallics 21 (2002) 2970.
[25] T.L. Schull, J.G. Kushmerick, C.H. Patterson, C. George, M.H. Moore, S.K. Pollack, R. Shashidhar, J. Am. Chem. Soc. 125 (2003) 3202.
[26] C. Olivier, B. Kim, D. Touchard, S. Rigaut, Organometallics 27 (2008) 509.
[27] H.M. Wen, Y. Yang, X.S. Zhou, J.Y. Liu, D.B. Zhang, Z.B. Chen, J.Y. Wang, Z.N. Chen, Z.Q. Tian, Chem. Sci. 4 (2013) 2471.
[28] Y. Tanaka, Y. Kato, T. Tada, S. Fujii, M. Kiguchi, M. Akita, J. Am. Chem. Soc. 140 (2018) 10080.
[29] L.Y. Zhang, P. Duan, J.Y. Wang, Q.C. Zhang, Z.N. Chen, J. Phys. Chem. C 123 (2019) 5282.
[30] A.S. Blum, T. Ren, D.A. Parish, S.A. Trammell, M.H. Moore, J.G. Kushmerick, G.-L. Xu, J.R. Deschamps, S.K. Pollack, R. Shashidhar, J. Am. Chem. Soc. 127 (2005) 10010.
[31] A.K. Mahapatro, J. Ying, T. Ren, D.B. Janes, Nano Lett. 8 (2008) 2131.
[32] F.B. Meng, Y.M. Hervault, Q. Shao, B.H. Hu, L. Norel, S. Rigaut, X.D. Chen, Nat. Commun. 5 (2014) 3023. Art.
[33] H. Zhu, S.J. Pookpanratana, J.E. Bonevich, S.N. Natoli, C.A. Hacker, T. Ren, J.S. Suehle, C.A. Richter, Q. Li, ACS Appl. Mater. Interfaces 7 (2015) 27306.
[34] N.F. Phelan, M. Orchin, J Chem. Educ. 45 (1968) 633.
[35] Z. Cao, T. Ren, Organometallics 30 (2011) 245.
[36] M.B. Nielsen, F. Diederich, Chem. Rev. 105 (2005) 1837.
[37] M. Gholami, R.R. Tykwinski, Chem. Rev. 106 (2006) 4997.
[38] Y. Zhao, R.R. Tykwinski, J. Am. Chem. Soc. 121 (1999) 458.
[39] Y.M. Zhao, K. Campbell, R.R. Tykwinski, J. Org. Chem. 67 (2002) 336.
[40] Y.M. Zhao, A.D. Slepkov, C.O. Akoto, R. McDonald, F.A. Hegmann, R.R. Tykwinski, Chem. Eur J. 11 (2005) 321.
[41] Y.M. Zhao, N.Z. Zhou, A.D. Slepkov, S.C. Ciulei, R. McDonald, F.A. Hegmann, R.R. Tykwinski, Helv. Chim. Acta 90 (2007) 909.
[42] K. Campbell, R. McDonald, M.J. Ferguson, R.R. Tykwinski, J. Organomet. Chem. 683 (2003) 379.
[43] K. Campbell, R. McDonald, M.J. Ferguson, R.R. Tykwinski, Organometallics 22 (2003) 1353.
[44] M.I. Bruce, A. Burgun, M.A. Fox, M. Jevric, P.J. Low, B.K. Nicholson, C.R. Parker, B.W. Skelton, A.H. White, N.N. Zaitseva, Organometallics 32 (2013) 3286.
[45] R. Makhoul, J.B.G. Gluyas, K.B. Vincent, H. Sahnoune, J.F. Halet, P.J. Low, J.R. Hamon, C. Lapinte, Organometallics 37 (2018) 4156.
[46] K.B. Vincent, J.B.G. Gluyas, Q. Zeng, D.S. Yufit, J.A.K. Howard, F. Hartl, P.J. Low, Dalton Trans. 46 (2017) 5522.
[47] Y. Fan, H.-M. Li, G.-D. Zou, X. Zhang, Y.-L. Pan, K.-K. Cao, M.-L. Zhang, P.-L. Ma, H.-T. Lu, Organometallics 36 (2017) 4278.
[48] Y. Fan, H.M. Li, G.D. Zou, X. Zhang, M. Li, J.H. Wu, H.T. Lu, J. Organomet. Chem. 859 (2018) 99.
[49] W.P. Forrest, Z. Cao, P.E. Fanwick, K.M. Hassell, T. Ren, Organometallics 30 (2011) 2075.
[50] W.P. Forrest, Z. Cao, K.M. Hassell, B.M. Prentice, P.E. Fanwick, T. Ren, Inorg. Chem. 51 (2012) 3261.
[51] W.P. Forrest, M.M.R. Choudhuri, S.M. Kilyanek, S.N. Natoli, B.M. Prentice, P.E. Fanwick, R.J. Crutchley, T. Ren, Inorg. Chem. 54 (2015) 7645.
[52] S.D. Banziger, T. Ren, J. Organomet. Chem. 885 (2019) 39.
[53] T. Ren, Chem. Commun. 52 (2016) 3271.
[54] W.P. Forrest, Z. Cao, R. Hambrick, B.M. Prentice, P.E. Fanwick, P.S. Wagenknecht, T. Ren, Eur. J. Inorg. Chem. (2012) 5616.
[55] Z. Cao, P.E. Fanwick, W.P. Forrest, Y. Gao, T. Ren, Organometallics 32 (2013) 4684.
[56] S.N. Natoli, T.D. Cook, T.R. Abraham, J.J. Kiernicki, P.E. Fanwick, T. Ren, Organometallics 34 (2015) 5207.
[57] S.N. Natoli, T.J. Azbell, P.E. Fanwick, M. Zeller, T. Ren, Organometallics 35 (2016) 3594.
[58] S.N. Natoli, M. Zeller, T. Ren, Organometallics (2019) (in press).
[59] W.A. Hoffert, M.K. Kabir, E.A. Hill, S.M. Mueller, M.P. Shores, Inorg. Chim. Acta 380 (2012) 174.
[60] S.N. Natoli, M. Zeller, T. Ren, Inorg. Chem. 56 (2017) 10021.
[61] S.D. Banziger, T.D. Cook, S.N. Natoli, P.E. Fanwick, T. Ren, J. Organomet. Chem. 799–800 (2015) 1.
[62] S.D. Banziger, X. Li, J. Valdiviezo, M. Zeller, D.N. Beratan, I. Rubtsov, T. Ren, Chem. Sci. (2019) (in preparation).
[63] M. Bruschi, M.G. Giuffreda, H.P. Luthi, Chem. Eur J. 8 (2002) 4216.
[64] B. Bosnich, C.K. Poon, M.L. Tobe, Inorg. Chem. 4 (1965) 1102.
[65] Gaussian 16, Revision B.01, Gaussian, Inc, 2016.
[66] G. Sheldrick, Acta Crystallogr. A 64 (2008) 112.